Particle gamma correlations in ^{12}C measured with the CsI(Tl) based detector array CHIMERA

G. Cardella [a,*], L. Acosta [a], F. Amorini [b], L. Auditore [d], I. Berceanu [h], A. Castoldi [g], E. De Filippo [a], D. Dell'Aquila [f], L. Francalanza [b,c], B. Gnoffo [a], C. Guazzoni [g], G. Lanzalone [b,e], I. Lombardo [f], T. Minniti [d], E. Morgana [d], S. Norella [d], A. Pagano [a], E.V. Pagano [b,c], M. Papa [a], S. Pirrone [a], G. Politi [a,c], A. Pop [h], L. Quattrocchi [d], F. Rizzo [b,c], E. Rosato [f,1], P. Russotto [a], A. Trifirò [d], M. Trimarchi [d], G. Verde [a], M. Vigilante [f]

[a] INFN - Sezione di Catania, Via S. Sofia, 95123 Catania, Italy
[b] INFN - Laboratori Nazionali del Sud, Via S. Sofia, Catania, Italy
[c] Dip. di Fisica e Astronomia, Università di Catania, Via S. Sofia, Catania, Italy
[d] INFN Gruppo collegato di Messina and Dip. di Fisica e Scienze della Terra, Università di Messina, Italy
[e] Facoltà di Ingegneria e Architettura, Università Kore, Enna, Italy
[f] Dipartimento di scienze Fisiche, Università Federico II and INFN Sezione di Napoli, Italy
[g] INFN Sezione di Milano e Politecnico Milano, Italy
[h] Institute for Physics and Nuclear Engineering, Bucharest, Romania

A B S T R A C T

The gamma decay of the first excited 4.44 MeV $2+$level of ^{12}C, populated by inelastic scattering of proton and ^{16}O beams at various energies was studied in order to test γ-ray detection efficiency and the quality of angular distribution information given by the CsI(Tl) detectors of the 4π CHIMERA array. The γ-decay was measured in coincidence with ejectile scattered particles in an approximately 4π geometry allowing to extract the angular distribution in the reference frame of recoiling ^{12}C target. The typical $\sin^2(2\theta)$ behavior of angular distribution was observed in the case of ^{16}O beam. Besides that, for the proton beam, in order to explain the observed distribution, the addition of an incoherent flat contribution was required. This latter is the effect of proton spin flip events allowing the population of $M=\pm 1$ magnetic substates, that is not possible in reactions induced by ^{16}O beam. A comparison with previously collected data, obtained measuring only in and out of plane proton-γ-ray coincidences, confirms the good quality of the angular distribution information given by the apparatus. Possible applications with radioactive beams are outlined.

1. Introduction

In nuclear reactions, inelastic scattering can be used to excite levels of projectile or target and gain information on their structure. At excitation energy lower than the particle threshold emissions, such levels decay trough γ-rays and their angular distribution, or angular correlation functions, can be used to get information on the level spin and parity and on the reaction mechanism involved in the reaction. In particular, by carefully choosing the reaction partners and detection geometry, one can observe polarization effects in order to pin down various terms of the nuclear effective interaction, as the intensity of the spin orbit potential (see for instance Ref. [1,2]). In this paper, aimed to prove the ability of our experimental system to detect discrete γ-rays, we revisit these effects by investigating the simple case of the ^{12}C (4.44 MeV) first excited level. It is well known that the 4.44 MeV is a 2^+ level decaying to ground state with E2 γ-transition decay [3,4]. We studied its population and decay, after inelastic scattering of both proton beams at 12, 15, and 18 MeV incident energy and ^{16}O beams at 10 A MeV. The observed differences between proton and ^{16}O projectiles induced reactions have been understood with respect to the ground state spins of the probes.

We used for the detection of both γ-rays and inelastic scattered beam particles the CHIMERA 4π multidetector [5]. This work is part of our effort to implement a valuable method of γ-rays-particles coincidence measurements, in reaction induced by in flight projectile fragmentation beams as available at Laboratori Nazionali del Sud (LNS) in Catania [6]. The final objective is to study the reaction mechanisms and the structure of nuclear systems populated with exotic beams [7].

* Corresponding author.
E-mail address: cardella@ct.infn.it (G. Cardella).
[1] Deceased.

Obviously, CHIMERA is essentially a 4π detector for charged particles and cannot compete, from the point of view of resolution, with very powerful germanium balls in construction as AGATA, or GRETA [8,9]) or even with less performing germanium arrays as for instance EXOGAM, MINIBALL, GASP/GALILEO, EXOGAM [10–12] or even with more specialized arrays with different material choices like DALI2, PARIS [13,14]. However due to the 4π coverage of the Si–CsI(Tl) telescopes and the simultaneous efficient detection of charged particles and γ-rays on such a large solid angle it could produce very interesting results, providing the adoption of appropriate detection requirements and methods. Essentially this last statement is described in the present paper. This paper is organized as follows: in Section 2, after a detailed description of the detector setup, we report on the angular distributions of γ-rays detected in p,p′ experiments; Section 3 is devoted to the data analysis of reactions collected with ^{16}O beam and to explain the difference in the measured angular distributions; in Section 4 we compare our results with previous investigations; perspectives and conclusions are discussed in Section5.

2. Detection system and p,p′ data

The experiment was performed at LNS in Catania by using the two accelerator facilities of this laboratory, the 15 MV tandem, and the superconducting cyclotron CS, to produce respectively protons and ^{16}O beams. The used detection system CHIMERA is a 4π apparatus, with 94% coverage of solid angle, built with 1192 double stage Si–CsI(Tl) telescopes [5]. CHIMERA was optimized to study multi-fragmentation reactions with particular emphasis on the timescale of the reaction and isospin observable [15]. To well cope with the needs of this physics case the detector was designed with a spherical part, made by 504 telescopes, covering the angles from 30° to 173° (in steps of 8° up to 150°), with a distance of 40 cm from the target, and a forward region, made by 688 telescopes, with much better granularity and a larger distance detector target (from 3.5 m at 1° to 1 m at 30°), allowing for more precise time of flight (TOF) measurements. The first stage of each telescope is a planar n-type silicon detector from 200 to 300 μm thick. The second stage is built with CsI(Tl) crystals coupled with read out Photodiodes and having thickness ranging from 12 cm, in most forward detectors, to 3 cm, at backward angles. Evidently, the CsI(Tl) stage of the telescopes is also suitable to detect γ-rays due to the high atomic number of the material producing a relatively large efficiency. Besides that, the presence of Thallium doping enables in fact γ-rays against charged particles discrimination by using various techniques [16–23]. The most useful part of CHIMERA, for γ-ray detection, is the CsI(Tl) stage of telescopes belonging to the spherical part of the detector. In fact, due to the larger solid angle coverage of the single detector and the smaller yield of charged particles, we can benefit of a larger signal to noise ratio. This will be very useful in the present data analysis, in fact the usual fast–slow analysis for γ-ray identification was not possible because of a missing stable time reference [16].

In Fig. 1 we plot the relative efficiencies to γ-rays of 4.44 MeV computed with Geant4 simulations for the CsI(Tl) of the spherical part of the detector as a function of the angle (Fig. 1a) and thickness (Fig. 1b). One can see that they range from 60% for 8 cm thick detectors, down to around 30%, for the 3 cm thick detectors of the most backward rings (for angles larger than 142°). Such efficiencies were computed summing first and second escape to photo peak. Small differences between detectors having the same thickness, but different shape, can be observed. They are due to changes in light collection efficiency. More in detail there is a change in the ratio between the detector surface and photodiode area and this is more effective for smaller thickness due to a less uniform diffusion of the light.

In the proton experimental campaign we irradiated a carbon target of 1 mg/cm^2 at 3 beam energies 12, 15 and 18 MeV. The data acquisition was triggered by the detection of the protons scattered in silicon detectors. To give an idea of the experimental conditions and collected statistics, in Fig. 2 we plot the number of protons collected at different angles and beam energies produced by inelastic excitation of the 4.44 MeV ^{12}C level (the lower contribution around 50°–60° is due to a large number of silicon detectors excluded by the analysis due to scarce trigger efficiency). The average total count rate in the most forward detectors around 30°, was not larger than 100 Hz. Protons were selected by putting a condition on the q-value spectra (3.5–5 MeV), see Fig. 3a. In order to search for γ-rays emitted from the decay of the 4.44 MeV excited level, we looked at CsI(Tl) data in coincidence with such protons. In Fig. 3b one can see the γ-energy spectrum obtained, under such condition, adding up all detectors at $82^\circ \pm 4^\circ$ (empty spectrum). Following GEANT4 simulations, the γ-energy calibration (in MeV electron equivalent MeVee) was obtained by assuming the energy of first escape (about 3.9 MeV) for the centroid of the peak. The background under this peak can be simply evaluated with the assumption that in coincidence with proton elastic scattering there cannot be γ-rays, but there is the same rate of spurious coincidences. The result of this background evaluation is plotted in Fig. 3b as green filled spectrum. It was normalized to the number of 4.44 inelastic scattering proton events. Its contribution to the peak area is less than 10% at this angle.

Integrating the peak observed in CsI(Tl) spectra (in the range 3–5 MeV), after background subtraction, we can extract the laboratory

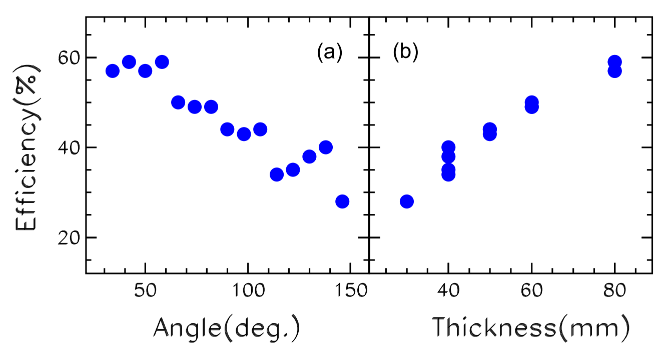

Fig. 1. CsI(Tl) efficiency to γ-rays of 4.44 MeV computed with Geant4 as a function (a) of detection angle, (b) of the thickness of scintillator.

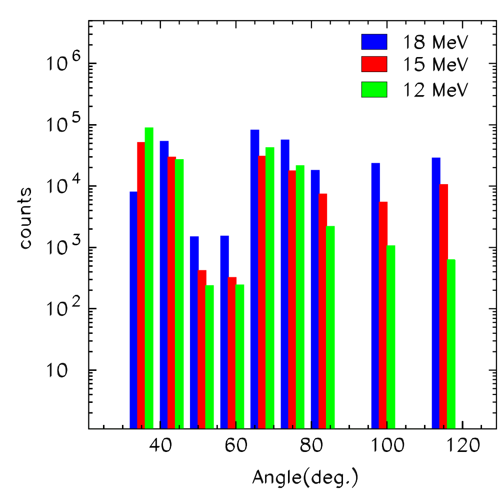

Fig. 2. Statistics of detected protons from inelastic excitation of the 4.44 MeV ^{12}C level.

angular distribution, plotted in Fig. 4a–c, for the three proton beam energies. Statistical error bars are smaller than the size of the symbols used. For comparison, in Fig. 4d, the angular distribution obtained by γ-rays produced after n,n′ scattering at 14 MeV on ^{12}C, adapted from Ref. [24], is also shown. In fact, due to the relatively small Coulomb field of protons and the identical spin of neutron and proton, the n,n′ data are expected to be very similar to all p,p′ data we have measured. Besides, due to the negligible role of the jacobian transformation from the Centre of mass (CM) system to laboratory (L) one, in both p,p′ and n,n′ data, we expect, for the observed transition, a nearly symmetry around 90° in the angular distribution. This symmetry ensures us that the quoted efficiency corrections (energy threshold effects have not been taken into account at this stage) account relatively well for both crystal size effects and geometrical inefficiencies of the whole apparatus. Efficiency corrections also take into account detectors excluded by the analysis for any problem, (all the 90° detectors, most detectors at 106°, and approximately 15% of the detectors of the other rings randomly distributed). The correct background subtraction is also essential to obtain this symmetric behavior. In fact in Fig. 5a we can see the rather

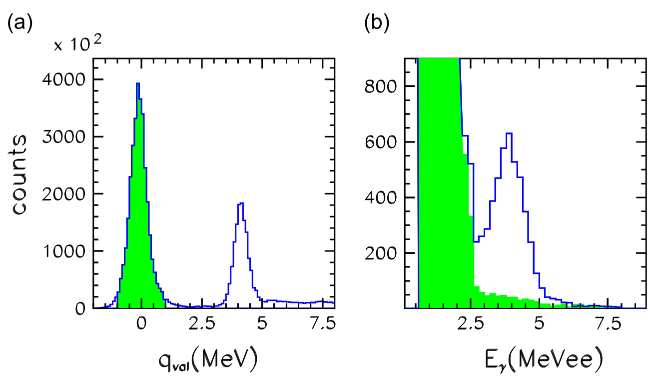

Fig. 3. (a)*q*-value spectrum generated in the p + ^{12}C reaction at 18 MeV. (b) Sum of calibrated CsI(Tl) energy spectra collected at 82° in the same reaction in coincidence with elastic scattering (filled histogram) and the 4.44 MeV peak (empty histogram). (For interpretation of the references to color in this figure, the reader is referred to the web version of this article.)

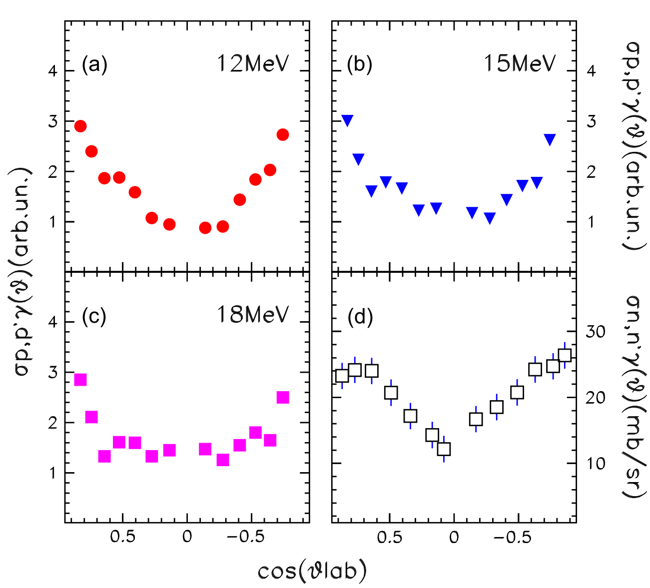

Fig. 4. (a)–(c) Laboratory γ-ray angular distribution from the decay of the 4.44 MeV ^{12}C level measured at the three different proton beam energies. d) Same angular distribution produced in n,n′ reaction on ^{12}C, adapted from Ref. [24]. (For interpretation of the references to color in this figure, the reader is referred to the web version of this article.)

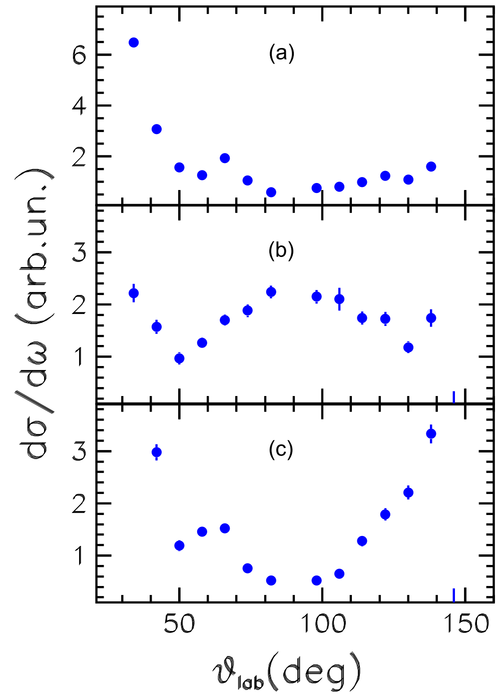

Fig. 5. γ-ray angular distributions: (a) background at 18 MeV proton energy; (b) in plane (c) out of plane p-γ coincidences from the ^{12}C$^{4.44}$.

asymmetric forward peaked angular distribution of background events. This is an obvious consequence of the larger count rate measured at forward angles, increasing the number of random coincidences.

However slightly different shapes and deepness of the minima around 90° measured at the three proton energies, as well as differences with respect to n,n′ data are present. Concerning the differences between p,p′ and n,n′ reactions, we notice that the two measurements have been performed in different ways. In the case of n,n′ reaction the trigger was simply given by detection of γ-rays (single counting). In our p,p′ reactions we had to trigger on protons (coincidence counting). The two set of data should be statistically consistent only in the case that the trigger efficiency was approaching the ideal value of 100%. However one bias in our experiment is that with increase of the proton energy the energy loss in silicon detectors decreases: as a consequence the trigger efficiency depends on the change of the electronic threshold. All the measurements reported here are in effect angular correlations between proton and γ-rays averaged over different proton effective angular distributions. As an example of how sensitive laboratory γ-rays angular distribution to proton trigger can be, in Fig. 5b and c we show what happens selecting only data with protons and γ-rays measured in the same plane (Fig. 5b) or in orthogonal planes (Fig. 5c). The opening angle is given by the ϕ-resolution of our detectors ± 6°. One sees that the shape of the distribution is very sensitive to plane selection, and small anomalies in the trigger efficiency in such planes can therefore affect the angular distributions shown in Fig. 4. As will be better seen in Section 4 this effect is connected to spin orbit interaction [1,2,25].

In order to recover from trigger effects and to sum coincidences from all detectors, maximizing statistics (useful for instance in the case of reactions induced by radioactive beams), one simple solution is to plot the angular distribution on the ^{12}C reference frame (CM of the recoiling system), choosing the ^{12}C recoil direction as the *Z* axis (see [26]). This task is simplified in our case because the velocity of the recoiling ^{12}C nuclei is so low that Doppler shift correction is negligible. To extract the correct CM angle, event by event, only rotations of the laboratory frame are necessary. Efficiency was evaluated with a MonteCarlo method, for each beam energy, using for the recoiling ^{12}C the distribution of emission angles. This angle was computed, assuming two-body kinematics, from the experimental distribution of scattered protons. A flat γ-ray angular distribution was assumed in MonteCarlo simulations, taking into account also for malfunctioning detectors excluded by the analysis. In Fig. 6a–c the CM γ-ray angular distributions are plotted for the three proton energies. For comparison and further check in Fig. 6e and f) angular distributions obtained integrating γ-ray spectra on the side of the main 4.44 MeV peak (respectively in the range 2–2.5 MeVee and 6–7 MeVee) are plotted. These off-gate distributions, taken at beam energy of 18 MeV, are rather different from the behavior of the main peak and relatively flat in the region from 50° to 120° confirming the quality of the obtained angular distribution. At larger angles the asymmetric behavior observed cannot be simply explained but can be affected also by small statistics and systematic errors, more important at such angles where the efficiency is smaller due to geometrical effects. All distributions are normalized to an average value of 1. We underline that, in the CM reference frame, the differences in the laboratory angular distributions measured at the three energies reported in Fig. 4 are much smaller. As reported in [26] CM angular distributions follow qualitatively the behavior predicted for E2 transition from the $M=0$ substate $\sin^2(2\theta)$ with a minimum around 90° and maxima around 45° and 135°. However to reproduce the experimental behavior (full lines) one also has to include a constant flat distribution (red dashed line, approximately of the same order of magnitude). It is possible that this flat contribution is at least partially due to a not well subtracted background, however this point will be better discussed in next sections and other more convincing explanations will be shown.

3. ^{16}O beam and comparison of the results

In order to further check the quality of the obtained angular distributions we decided to look more in detail for entrance channel spin effects. We therefore analyzed other CHIMERA data, measured using a zero spin projectile, as the ^{16}O. In particular we show here data taken using ^{16}O beam at 10 A MeV on carbon target. For this experiment a thinner target of about 50 μg/cm^2 was used to minimize effects due to beam energy loss. In these reactions we can see both the 4.44 γ – decay and the decay of the group of levels around 6–7 MeV from ^{16}O excitation. In Fig. 7a and b q-value spectra, evaluated from the scattered ^{16}O particles detected near the grazing at 5.2° and 6.4° average angles are reported (all CHIMERA detectors of a ring are summed in these spectra, a resolution of about 1 MeV can be evaluated mainly due to kinematics). Filled regions of the spectra corresponding to the 4.44, 6–7 MeV and elastic scattering peaks have been evidenced, with different styles, in order to clarify the presentation. In Fig. 7c and d the γ-ray spectra obtained by gating with the different q-value windows, shown in Fig. 7a andb, and summing the CsI(Tl) signals from all the detectors of ring 14 (66° ± 4°) are shown (the filling style used in panels a, b identify the adopted cut). More in detail events with ^{16}O particles at 5.2° and 6.4° inside the cuts relative to the 4.44 MeV ^{12}C level are added in Fig. 7c, while in Fig. 7d events with ^{16}O particles at 6.4° inside the cut relative to the 6–7 MeV ^{16}O levels are added. Also in this case the level of background under the γ-peak was evaluated by looking to spurious coincidences with elastic scattering data, and normalizing it to the number of inelastic scattering events. The two γ-ray peaks around 4 and 6 MeV, selected respectively in coincidence with the 4.44 and 6-7 MeV q-value windows, are very well observed thanks to the cleaning effect produced by particle-γ-ray coincidence. In the experiment reported here the group of γ-rays at around 6 MeV (levels of ^{16}O at 6, 6.1, 6.9 and 7.1 MeV [3]) has not been discriminated due to the limited CsI(Tl) energy resolution and, consequently, they were not further analyzed. The angular distribution of 4.44 MeV γ-rays was still evaluated in the CM of the recoiling ^{12}C. Again Doppler shift correction has been neglected. Results are plotted in Fig. 6d, compared to the angular distributions obtained with proton beams (Fig. 6a–c). We note immediately that the 90° minimum, in the case of ^{16}O beam, is much deeper and goes down to vanishing values close to zero. Consequently only 10% constant flat component was summed to $\sin^2(2\theta)$ contribution in the plotted curve. Maxima are larger than expected from the simple $\sin^2(2\theta)$ behavior, we do not have simple explanation for this. However, as reported above, at small (< 40°) and large angles (> 140°), due to geometrical effects, efficiency is smaller and systematical errors could be more important.

Because background was evaluated and subtracted from data with proton and oxygen beam in the same way we can exclude that the flat contribution added to $\sin^2(2\theta)$ behavior is generated

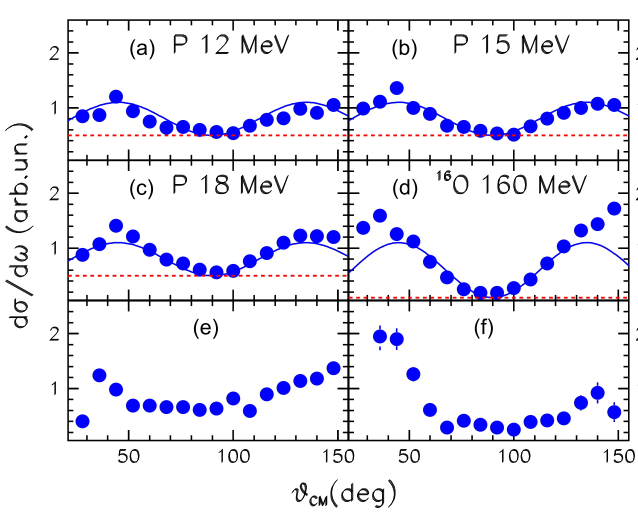

Fig. 6. γ-ray angular distributions of the 4.44 MeVee peak in the CM of the recoiling ^{12}C measured with proton (a),(b),(c) and ^{16}O beams (d). Lines are discussed in the text. (e),(f) same as (c) but with γ-energy windows lower (2–2.5 MeVee) and upper (6–7 MeVee) than the 4.44 MeVee peak.

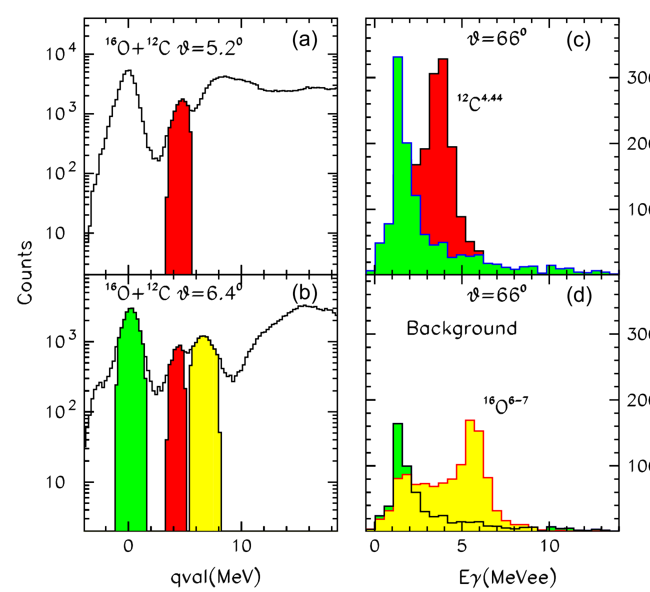

Fig. 7. (a),(b) q-value spectra measured with ^{16}O + ^{12}C reaction near the grazing angle. (c),(d) γ-ray spectra detected at 66° in coincidence with different q-value windows.

by not correctly evaluated background. To investigate better about this difference in the deepness of the minima, we can also compare the two different sets of data with respect with the different target kinematics. One notes that we measured with a better angular resolution the ^{16}O inelastic scattering (measured at very forward angles with $\Delta\theta \approx 1$–2°) than the proton one (measured at larger angles with angular resolution of $\pm 4^\circ$). However, the different kinematics of the target using heavy and light projectiles, does not change, within experimental resolution, the spread in the evaluation of the ^{12}C recoiling angle that remains in both cases well inside the angular resolution of scintillator detectors. A second, perhaps more important, difference in the two experiments was the target thickness used. In the ^{16}O experiment the target was thin enough to allow ^{12}C* recoils to escape. In contrast in the proton experiment the ^{12}C* recoiling nuclei were stopped in most cases in the target (1 mg/cm^2 equivalent to 4 μm). It is obvious that, if the γ-rays are emitted from a ^{12}C* at rest, or near the end of its Bragg peak, the original recoil direction is lost; therefore, the angular distribution with respect to this axis will be averaged with respect to the emission time. We notice that the width of the 4.44 level is relatively small, from NNDC database [3] 10.8×10^{-3} eV (this width was measured with inelastic scattering of electrons, see for instance [27]). So from Heisemberg uncertainty relation, a lifetime of $T \approx \hbar/\Delta E = 0.06$ ps is evaluated. Assuming 1 MeV as typical carbon recoiling energy (approximate range in Carbon 1.2 μm), a calculation assuming a constant deceleration shows that one needs about 10 lifetimes before ^{12}C is fully stopped in the target. Therefore most decays happen when ^{12}C is still moving and preserving the original direction with angular straggling small with respect to detector resolution. We argue that the target thickness cannot be either responsible for the smoothing of the γ-ray angular distributions observed with proton beams. In conclusion, our analysis shows that the observed difference between p and ^{16}O data is not consistent with the different experimental conditions of the two experiments.

One can find a simple solution to the difference in the observed γ-ray angular distributions by looking at angular momentum conservation rules. In the reaction with ^{16}O we have all particles involved with zero spin, while proton is a spin ½ particle. For the total angular momentum conservation, in a semi-classical picture, one can see that for the case of ^{16}O beam we have:

$$\mathbf{J_1} = \mathbf{I_{12C}} + \mathbf{L_1} + \mathbf{I_{O16}} = \mathbf{L_1} \quad \mathbf{J_2} = \mathbf{I_{12C^*}} + \mathbf{L_2} + \mathbf{I_{O16}} = \mathbf{I_{12C^*}} + \mathbf{L_2} \text{ and because } \mathbf{J_1} = \mathbf{J_2} \text{ then } \mathbf{I_{12C^*}} = \mathbf{\Delta L}$$

with $\mathbf{J}$ being the total angular momentum in the entrance (1) and outgoing (2) channels, $\mathbf{L}$ the relative angular momentum $\mathbf{\Delta L = L_1 - L_2}$ and $\mathbf{I_x}$ the spin of the x nucleus, (bold notation indicate vector quantities).

Both $\mathbf{L_1}$ and $\mathbf{L_2}$ are by definition orthogonal to the reaction plane, so $\mathbf{\Delta L}$ is aligned perpendicularly to ^{12}C* direction (chosen as Z axis) and $M_{12C^*} = 0$.

In the case of proton beams, because of the proton spin, we have a more complex case as follows:

$$\mathbf{J_1} = \mathbf{I_{12C}} + \mathbf{L_1} + \mathbf{I_p} = \mathbf{L_1} + \mathbf{I_p} \quad \mathbf{J_2} = \mathbf{I_{12C^*}} + \mathbf{L_2} + \mathbf{I_p} = \mathbf{I_{12C^*}} + \mathbf{L_2} + \mathbf{I_p} \text{ and because } \mathbf{J_1} = \mathbf{J_2} \text{ therefore } \mathbf{I_{12C^*}} = \mathbf{\Delta L} + \mathbf{\Delta I_p}$$

Clearly because we expect proton spin flip events, due to spin orbit interaction [1,2], in this case the values ± 1 are allowed for M_{12C^*}. The effect of the population of such magnetic substates seems, in our data, a less pronounced minimum in the angular distribution at 90° as observed in Fig. 6. In next paragraph we will further discuss this point.

4. Other methods to observe spin flip probability

The choice of the reference frame of the recoiling system is quite useful, in case of low statistics, because one can sum data from all available detectors. However other reference frames are possible, and were largely used in the past (see for instance [1,2,25,28–30]). We will shortly describe the similarities of these approaches. In Ref. [1] for instance two γ-ray detectors were used with opportune lead shield for in and out of plane measurements while an array of si-lithium drifted was used as proton detectors. When mounted in plane, proton and γ-ray detectors were mounted on opposite sides. The reference frame was chosen as the Laboratory frame, with the Z axis given by the vector product of the beam axis and of the proton direction. The X axis was chosen along the beam direction, therefore, in this frame, the polar angles θ_{lab}, reported in Figs. 4 and 5 are called azimuthal angles ϕ_{lab} and vice versa. To avoid confusion we will continue to use the notation up to now used, therefore the angular correlation of γ-rays (Ref. [1], Eq. (7)) can be rewritten as follows:

$$W(\phi_{plab} = 1/2\pi,\ \theta_{plab};\ \phi_{\gamma lab} = -1/2\pi, \theta_{\gamma lab}) = (5/16p)*(A + B\sin^2 2(\theta_{\gamma lab} - \varepsilon_2) + C\sin^2(\theta_{\gamma lab} - \varepsilon_1)) \quad (1)$$

In Ref. [1] the A, B, and C coefficients are related to the populations s_0, s_1, and s_2 of magnetic substates 0, ± 1, and ± 2 respectively of ^{12}C* (spin projections along the above chosen Z axis perpendicular to reaction plane, note that this is orthogonal to the beam direction chosen as Z axis in par.2,3). In order to extract these populations, as a function of the proton scattering angle, it is also essential to measure the so called Z axis correlation function W ($\phi_p = 1/2\pi$, θ_{plab}; $\phi_{\gamma lab} = 0$) so that from Ref. [1], Eq. (10) is proportional to s_1 population. The knowledge of s_1 allows in fact unambiguous extraction of s_0 and s_2 values from the fit parameters A, B and C. Unfortunately, due to some bias malfunction of the 90° ring, that was excluded by the analysis, the statistics of our measurement is not enough to perform a complete analysis in this framework. However, we can compare our data with the ones of Ref. [1] proving that the two approaches are identical. In Fig. 8a we plot the correlation function measured selecting protons detected at 66° in the lab (around 71° in CM of the binary reaction), and γ-rays on the opposite side of the reaction plane (following the geometry of Ref. [1]). Data are collected at 18 MeV proton beam energy to be more similar to the 20 MeV beam energy investigated in Ref. [1]. In the figure we also plot, as full line, Eq. (1) and its three contributions (dot line the constant factor A, dashed line the term $B\sin^2 2(\theta_{\gamma lab} - \varepsilon_2)$, and full histogram of the last term $C\sin^2(\theta_{\gamma lab} - \varepsilon_1)$, very small). We used the A, B, and C parameters, obtained from the fits of Ref. [1], scaled to take into account for the different normalizations. For A parameter, to better

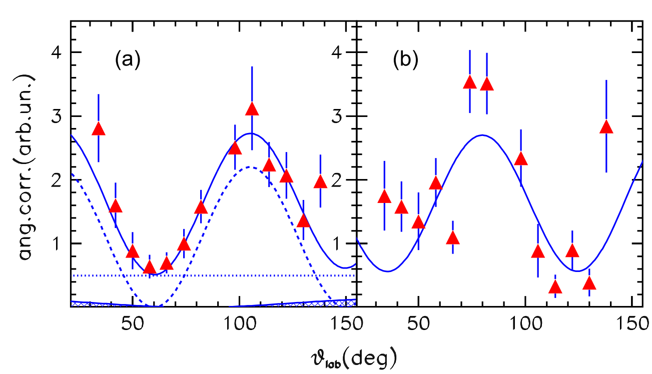

Fig. 8. Angular correlations of γ-rays detected in coincidence with protons (a) on opposite side of the reaction plane; (b) on the same side of the reaction plane. Lines are computed with Eq. (1), see text.

reproduce the minimum value of experimental data, we used the lower limit given by the error bar. We also had to slightly adjust the ε_2 parameter from 51° to 60°. We see that the weight of the last term in C is negligible, the dominant terms are the constant A factor, determined by the amplitude of the minimum of correlation function, and the term in $B\sin^2 2(\theta_{\gamma \mathrm{lab}}-\varepsilon_2)$. For this term the ε_2 value determines the phase of the oscillation. The similarity of this fitting expression with the one used to reproduce data in Fig. 6 is striking. On the other hand, when the detectors are in the reaction plane, and Doppler shift can be neglected, the θ_{cm} angle in the recoiling nucleus system is just the difference between $\theta_{\mathrm{lab}\gamma}$ and θ_{recoil}. We can simply conclude that the ε_2 angle should be equal to θ_{recoil} (as also indicated in some approximated expression in [30]).This is true neglecting the effects of Fermi motion of nucleons and the finite opening angle of detectors. Under these latter assumptions we used a fit parameter around 60° while the average θ_{recoil} is 48°. In Fig. 8b we plot the angular correlation measured detecting both protons and γ-rays on the same side of the reaction plane. In this case we have to add to $\theta_{\mathrm{lab}\gamma}$ the recoil angle to get the CM angle and so, we get the fit parameter +55° to reproduce the position of the maximum, that is rather similar to the expected θ_{recoil} value. Looking to panels a and b of Fig. 8 one simply understands why the in plane coincidences plotted in Fig. 5b have a maximum around 90°. This behavior is due to the sum of out of phase oscillations (note however that Fig. 5b was extracted summing data collected at all proton detection angles, while Fig. 8 is obtained by looking only to protons detected at 66°).

Clearly if the statistics of the experiment is good enough (with respect to the overall resolution), the best way to extract quantitative information on spin flip probability and therefore on spin orbit interaction is to measure the in plane and out plane particle-γ correlation functions. However we have shown, in well-known physical case, that the same information, are also available, by integrating over the measured particle scattering angles, from the amplitude of minima in correlation functions measured in the reference frame of the emitting nucleus. This latter equivalence can be very useful for investigation with low intensity exotic beams.

5. Perpesctives and conclusions

This work shows the capability of the CHIMERA detector to extract meaningful angular distributions from high energy γ-rays. With such a powerful detector a nearly complete spin alignment was observed looking to angular distribution of γ-rays emitted from the decay of the 4.44 MeV first excited state of ^{12}C when populated by inelastic scattering of ^{16}O nuclei. A smaller polarization was observed using proton beams from 12 to 18 MeV. We have excluded possible experimental bias due to the better angular resolution measurement of the triggering ^{16}O, and to the thicker target used for the proton runs. The smaller polarization is due to the population of ^{12}C magnetic substates $M=\pm 1$ allowed by angular momentum conservation in case of proton spin flip events. This effect can be used as a complementary way, with respect to elastic scattering, to study the intensity of spin orbit interaction responsible for the proton spin flip process. Often, as in Ref. [1,2,28,29], this was done by using a simple dedicated set-up with detectors for particles and γ-rays mounted in both in and out-plane configurations. The 4π geometry used in this work has the advantage to allow the sum of various in and out plane detector combinations, or, in case of very small statistics, to sum data from all available detectors, irrespective of their detection plane. This last option can be very useful in case of reactions with radioactive beams where, due to scarce statistics, one has to use all possible coincidences data with large solid angle arrays.

We plan to use in future experiments the CsI(Tl) of CHIMERA in order to detect γ-rays in reactions induced by fragmentation radioactive beams at LNS. The γ-ray detection will be useful to disentangle reactions leading to ground state from inelastic channels. We will also try, in selected cases, to extract information on spin flip processes and on the spin orbit interaction with exotic nuclei.

Thanks are due to F. Crespi, J.J. Valiente Dobon, and F. Camera for stimulating discussions about γ-ray detection and the analysis of these results.

References

[1] J.R. Tesmer, F.H. Schmidt, Physical Review C 5 (1972) 864.
[2] M. Tanaka, J. Kawa, T. Fukuda, T. Shimoda, K. Katory, S. Nakayama, I. Miura, H. Ogata, Physics Letter 106B (1981) 293.
[3] ⟨http://www.nndc.bnl.gov/⟩.
[4] F. Ajzenberg-Selove, Nuclear Physics A 506 (1990) 1.
[5] A. Pagano, et al., Nuclear Physics A 734 (2004) 504;
A. Pagano, Nuclear Physics News 22 (1) (2012) 25;
E. De Filippo, A. Pagano, European Physical Journal A 50 (2014) 32.
[6] I. Lombardo, et al., Nuclear Physics B - Proceedings Supplements 215 (2011) 272;
G. Raciti, E. Rapisarda, M. De Napoli, F. Amorini, L. Calabretta, G. Cardella, G. Cosentino, C. Sfienti, V. Shchepunov, Nuclear Instruments and Methods B 266 (2008) 4632.
[7] L. Acosta, et al., Nuclear Instruments and Methods A 715 (2013) 56;
G. Cardella, et al., European Physical Journal Web of Conference 66 (2014) 03016.
[8] E. Farnea, et al., Nuclear Instruments and Methods A 621 (2010) 331.
[9] M.A. Deleplanque, et al., Nuclear Instruments and Methods A 430 (1999) 292.
[10] M. Petri, et al., Nuclear Instruments and Methods A 607 (2009) 412.
[11] N. Warr, et al., European Physical Journal A 49 (2013) 40.
[12] D. Mengoni, F. Recchia, J.J. Valiente Dobon, LNL Annual Report 2013 (2013) 68.
[13] ⟨http://www.nishina.riken.jp/collaboration/SUNFLOWER/devices/dali2/index.html⟩.
[14] ⟨http://paris.ifj.edu.pl/index.php?lng=en⟩.
[15] E. De Filippo, et al., Physical Review C 71 (2005) 044602;
E. De Filippo, et al., Physical Review C 86 (2012) 014610;
M. Papa, et al., Physical Review C 91 (2015) 041601;
F. Amorini, et al., Physical Review Letters 102 (2009) 112701;
G. Cardella, et al., Physical Review C 85 (2012) 064609;
I. Lombardo, et al., Nuclear Physics A 834 (2010) 458;
P. Russotto, et al., Physical Review C 91 (2015) 014610.
[16] M. Alderighi, et al., Nuclear Instruments and Methods A 489 (2002) 257.
[17] W. Skulski, M. Momayezi, Nuclear Instruments and Methods A 458 (2001) 759.
[18] M. Bendel, R. Gernhäuser, W.F. Henning, R. Krücken, T. Le Bleis, M. Winkel, European Physical Journal A 49 (2013) 69.
[19] J. Pouthas, et al., Nuclear Instruments and Methods A 357 (1995) 418.
[20] M. Parlog, et al., Nuclear Instruments and Methods A482 (2002) 674.
[21] D.G. Sarantites, P.-F. Hua, M. Devlin, L.G. Sobotka, J. Elson, J.T. Hood D.R. LaFosse, J.E. Sarantites, M.R. Maier, Nuclear Instruments and Methods A 381 (1996) 418.
[22] F. Amorini, et al., IEEE Trans. On Nucl. Sci. 59 (2012) 1772.
[23] L. Acosta, et al., IEEE Transactions on Nuclear Science 60 (2013) 284.
[24] J. Benveniste, A.C. Mitchell, C.D. Schrader, J.H. Zenger, Nuclear Physics 19 (1960) 448.
[25] F. Rybicki, T. Tamura, G.R. Satchler, Nuclear Physics A 146 (1970) 659;
G.R. Satchler, Direct Nuclear Reactions International Series of Monographs on Physics, Oxford University Press, New York, USA (1983) 377.
[26] J.R. Beene, F.E. Bertrand, M.L. Halbert, R.L. Auble, D.C. Hensley, D.J. Horen R.L. Robinson, R.O. Sayer, T.P. Sjoreen, Physical Review C 39 (1989) 1307.
[27] Hall Crannel, T.A. Griffy, L.R. Suelzle, M.R. Yearian, Nuclear Physics A 90 (1967) 152.
[28] R. De Leo, G. D'Erasmo, F. Ferrero, A. Pantaleo, Nuclear Physics A 212 (1973) 253.
[29] W. Dünnweber, P.D. Bond, C. Chasman, S. Kubono, Physical Review Letters 43 (1979) 1642.
[30] F.H. Schmidt, R.E. Brown, J.B. Gerhart, W.A. Kolasinski, Nuclear Physics 52 (1964) 353.